CHEMICAL LASERS

The *laser,* an abbreviation for light amplification by stimulated emission of radiation, is a source of nearly monochromatic, coherent, electromagnetic radiation that propagates as a beam. The *chemical laser* is a type of laser system that is driven by the release of energy during a chemical reaction. Chemical lasers are usually large, high-power devices that integrate chemical delivery systems, a supersonic flow apparatus, and an optical resonator.

The light from a laser differs in several significant ways from the light from an ordinary incandescent bulb. The electromagnetic waves emitted by an ordinary source have many different wavelengths, or colors, and often appears "white." Furthermore, these waves are uncoordinated in that their crests and valleys exhibit no well-defined pattern with respect to each other. Finally, emission from individual points from within the ordinary source propagates in all directions. In contrast, laser light possesses a well-defined color (monochromatic), the waves are coordinated with crests and valleys in phase with each other (coherent), and the light propagates in a well-defined direction (as a beam).

The physical process by which laser light is generated is termed *stimulated emission* and was discovered by Albert Einstein in 1916. Light can interact with matter through several processes, including absorption, spontaneous emission, and stimulated emission as shown in Fig. 1. Consider a material with several states of quantized internal energy, E_0, E_1, and E_2. In thermal equilibrium, most of the atoms or molecules are in the state of lowest energy. This situation is illustrated with a large number of open circles populating the energy level E_0. When light is incident on such a material, as illustrated by the wave packet, the intensity may be attenuated as it is transmitted through the material via the process of absorption. The energy associated with the attenuated light is deposited into the material and some of the atoms or molecules transition to a state of higher energy, E_2. The particle undergoing this transition is shaded grey in the initial state and black in the final state of Fig. 1.

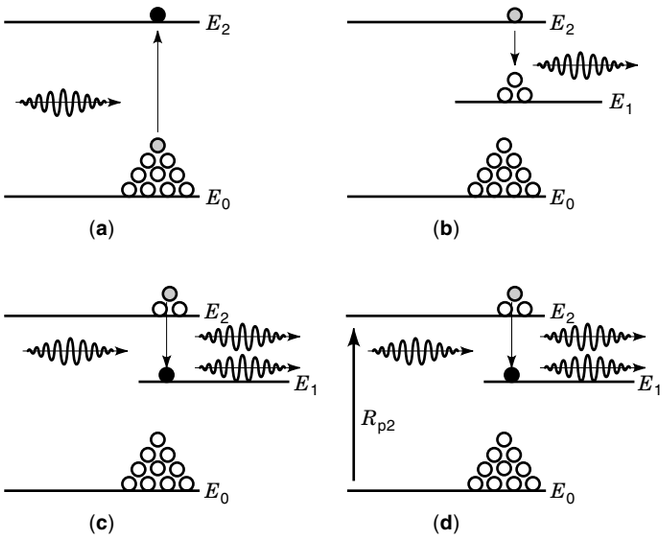

Figure 1. The interaction of light with matter via (a) absorption, (b) spontaneous emission, and (c) stimulated emission. Pumping of an excited state to produce a population inversion is shown in (d).

The light emitted from an ordinary source is generated by spontaneous emission. If an atom or molecule is in an excited state, E_2, one of the ways it can decay to a state of lower energy, E_1, is by emission of a photon. The photon is a packet of light with energy equal to the difference in energy between the emitting and final states. The frequency of the emitted light, ν, is related to the energy difference, $E_2 - E_1$, by Planck's constant, $h = 6.6256 \times 10^{-34}$ J · s:

$$\nu = (E_2 - E_1)/h \tag{1}$$

The frequency and wavelength λ of light propagating in a vacuum are related by the speed of light, $c = 2.9979 \times 10^8$ m/s:

$$\lambda\nu = c \tag{2}$$

Spontaneous emission occurs without external influence and is independent of other emission from within the sample [see Fig. 1(b)].

Alternatively, emission may be stimulated by an incident photon. In this stimulated emission process, the newly emitted photon possesses the same energy, direction of propagation, and phase as the incident photon. An exact copy of the incident photon is generated and the intensity of the light is amplified as the wave continues to propagate through the medium. This is the mechanism by which laser light is generated and is illustrated in Fig. 1(c).

Both stimulated emission and absorption will occur between a pair of energy levels. Normally, there are more atoms and molecules in the lower-energy state, and the rate for absorption is greater than stimulated emission. Under these circumstances, light is attenuated as is propagates through the medium. However, if there are more atoms or molecules in the level of higher energy, then stimulated emission will dominate and amplification of the incident light may be achieved. Thus, a population inversion between the two energy levels is required to produce a laser. To achieve this population inversion, the medium must be "pumped" by an external source to selectively deposit energy in the upper laser level, E_2. This laser pumping, or excitation, is shown schematically in the last segment of Fig. 1.

It was not until 1960 that T. H. Maiman used these ideas and demonstrated the first laser device, the ruby laser. A laser typically consists of an energy source, a gain medium, and an optical resonator, as shown in Fig. 2. The energy source is required to disturb the sample of atoms or molecules from equilibrium and pump the upper laser level. The gain medium provides for the amplification of light, which initially arises from spontaneous emission from within the sample. The optical resonator is usually a set of mirrors that provide

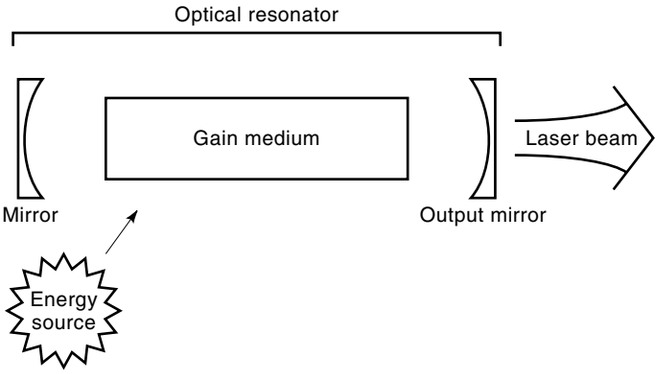

Figure 2. A laser is typically composed of three major components: a gain medium where the light is amplified, an external energy source to produce the population inversion, and an optical resonator or laser cavity which provides feedback to the gain medium and establishes a well-defined laser beam.

feedback of light for multiple passes through the gain medium to establish an intense beam of radiation. Considering the light within the optical resonator as an electromagnetic wave, one can see that the wave must replicate its phase upon a round-trip for the two wave trains to interfere constructively. Thus, the optical resonator may be designed to select a single mode and produce nearly monochromatic radiation.

The development of the laser represents a significant scientific and technical achievement. In 1964 the Nobel Prize in physics was awarded to C. H. Townes, N. G. Basov, and A. M. Prokhorov for their fundamental work in quantum electronics, particularly leading to the construction of the laser.

THE CHEMICAL LASER

The chemical laser depends on the energy liberated from an exothermic chemical reaction to produce the population inversion. Polanyi first proposed a chemical laser in 1960 by recognizing that many chemical reactions deposit excess energy in the stretching vibrations of the newly formed bond (1). If the chemical reaction favors the production of states with greater internal energy over states with less internal energy, then a population inversion can be achieved.

As an example of using a chemical reaction to pump a laser, consider the reaction of atomic fluorine with molecular hydrogen to produce vibrationally excited hydrogen fluoride, as shown in Fig. 3. This reaction produces 130 kJ/mol excess energy, which can be deposited in vibration of the newly formed HF bond (2). The first four vibrational levels, $v = 0$ to 3, are accessible. The barrier to this reaction is small, 5 kJ/mol, and thus the rate for producing HF is quite rapid. The key to developing an HF laser based on this reaction is the relative rates for producing the various vibrational levels of HF. These relative rates have been measured as 12 : 20 : 6 : 1 for $v = 3 : 2 : 1 : 0$ (3). Thus, 31% of the HF products will be found in the vibrational level $v = 3$. The most probable product is $v = 2$ at 51%. Only 3% of the reactions yield the lowest vibrational state, $v = 0$. Clearly, a population inversion between vibrational levels in HF can be generated by this direct chemical reaction.

In 1965 Kasper and Pimentel demonstrated the first chemical laser by initiating a hydrogen–chlorine explosion with a flashlamp (4). Within a few years, purely chemical, continuous-operation HF lasers based on the chemistry described previously had been demonstrated and by 1984 HF lasers with powers greater than 1 MW were developed (5). The HF chemical laser operates in the infrared region near a wavelength of 2.7 μm.

The basic components of a combustion-driven, supersonic mixing HF laser are shown in Fig. 4. Fluorine atoms must be produced to drive the $F + H_2 \rightarrow HF + H$ reaction, and this is accomplished by thermal dissociation of molecular fluorine at high pressure and temperature in the combustor. Typically, molecular deuterium is injected as the fuel and burned with molecular fluorine or NF_3 to produce 30% to 50% dissociation of F_2 at 2000 K to 4000 K and 1 kPa to 15 kPa total pressure. These temperature and pressure conditions are far too high for efficient laser operation, and the effluents of the combustor including the atomic fluorine are supersonically expanded through a nozzle assembly at Mach 1 to 3, producing a temperature of 300 K to 500 K and a pressure of 0.2 kPa to 0.8 kPa in the gain region. While the flow is cooled, the fluorine atoms remain dissociated as there is insufficient time for recombination to molecular fluorine. Molecular hydrogen is then injected into this supersonic expansion through a large number of very small nozzles to enable good mixing and efficient reaction with the atomic fluorine to produce the vibrationally inverted HF molecules for lasing. Another function of the supersonic flow is stretching of the reaction zone for the $F + H_2 \rightarrow HF + H$ reaction over the full width of the laser resonator. The laser cavity is formed so that the laser beam propagates in a direction perpendicular to the gas flow. Finally, the diffuser is designed to recover as much of the inlet stagnation pressure as possible before exiting to the mechanical or steam injection vacuum pumping system where the gases are exhausted.

The DF chemical laser substitutes deuterium for hydrogen to react with the atomic fluorine, F + D2 → DF + D, and

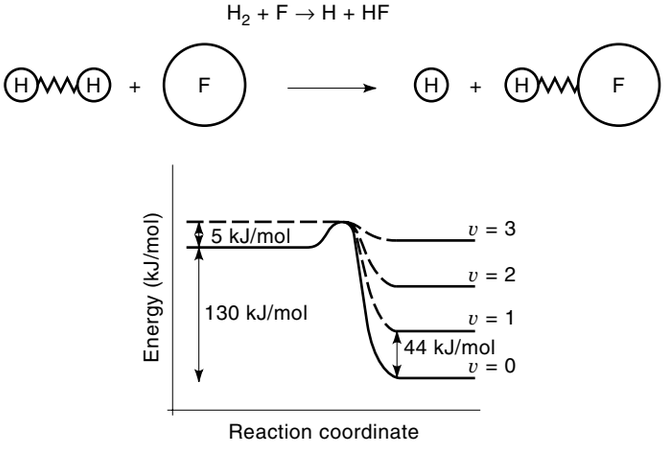

Figure 3. The reaction of atomic fluorine with molecular hydrogen produces vibrationally excited hydrogen fluoride. The reaction coordinate represents the breaking of the H_2 bond as the fluorine atom approaches and the subsequent formation of the HF bond as the product hydrogen atoms departs the collision center.

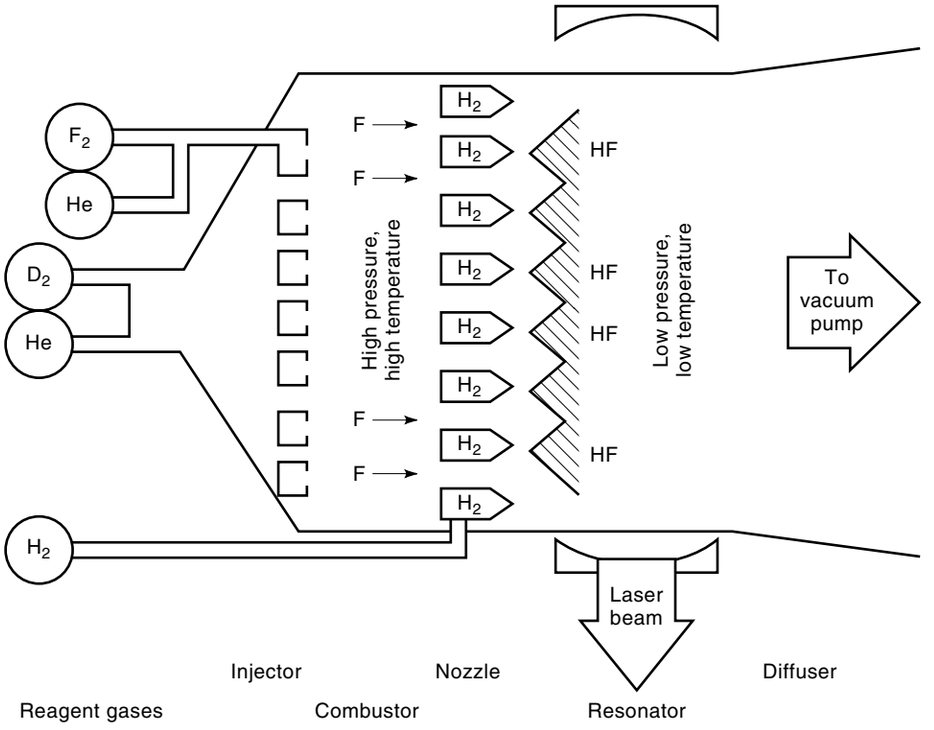

Figure 4. Schematic diagram of a typical supersonic mixing hydrogen fluoride chemical laser.

uses hardware very similar to the HF laser. The vibrational energy for DF is less than HF, and the DF laser operates at a wavelength near 3.8 μm. The atmosphere exhibits a window with good transmission at 3 to 5 μm, making the DF laser the preferred one for applications requiring atmospheric propagation.

CHEMICAL LASER PERFORMANCE

Several key parameters that describe the performance of a chemical laser are defined in Table 1. The laser gain γ is specified by the product of the cross-section for stimulated emission σ and the population inversion Δ:

$$\gamma = \sigma\Delta = \sigma[N_2 - (g_2/g_1)N_1] \tag{3}$$

where N_2 and N_1 are the concentrations and g_2 and g_1 are the degeneracies for the upper and lower laser levels, respectively. The upper and lower laser levels are labeled by their energies, E_2 and E_1, in Fig. 1. The cross section for stimulated emission is related to the spontaneous emission rate:

Table 1. Chemical Laser Performance Parameters

		Typical Value	
Laser Parameter	Symbol	HF Laser	COIL
Wavelength	λ	2.7 μm	1.3 μm
Gain	γ	20 %/cm	1 %/cm
Mass efficiency	σ_m	150 kJ/kg	300 kJ/kg
Nozzle flux	δ	· · ·	200 kW/cm^2
Beam quality	BQ	2	1.3
Saturation intensity	I_{sat}	0.1 kW/cm^2	5 kW/cm^2

$$\sigma = A_{21}(\lambda_0^2/8\pi)g(\lambda) \tag{4}$$

where A_{21} is the rate for spontaneous emission from level E_2 to level E_1 (s^{-1}), the laser wavelength $\lambda_0 = hc/(E_2 - E_1)$ (nm), and $g(\lambda)$ is the line shape function, specifying the shape and width of the spontaneous emission centered at wavelength λ_0 (s).

Typically, the total pressure in the gain region of a chemical laser is low and the transition is inhomogeneously broadened with a Gaussian line-shape function:

$$g(\lambda) = \sqrt{\frac{4\ln 2}{\pi}}\left(\frac{1}{\Delta\nu_D}\right)\exp\left[-4\ln 2\left(\frac{c/\lambda - c/\lambda_0}{\Delta\nu_D}\right)^2\right] \tag{5}$$

where the Doppler linewidth $\Delta\nu_D = \sqrt{8kT\ln 2/Mc^2}\,(c/\lambda_0)$ (Hz), Boltzmann's constant $k = 1.3805 \times 10^{-23}$ J/K, T is the gas temperature (K), and M is the mass per emitter particle (kg).

When the gain exceeds the total optical losses, α, due to mirror output coupling, scattering losses, and resonator losses, then net amplification and lasing may be achieved. The threshold population inversion is defined as the inversion required for the gain to equal the losses, $\gamma_{th} = \alpha$, or

$$\Delta_{th} = \alpha/\sigma \tag{6}$$

The HF laser exhibits high gain, which enables the design of optical resonators with large output coupling. However, large gain also limits the length of the cavity, as large amplification can be established without many round trips in the cavity. Such a situation leads to amplified spontaneous emission without good beam quality and coherence properties. Low-gain lasers operate nearer threshold and optical losses more significantly diminish efficiency but allow for longer-gain me-

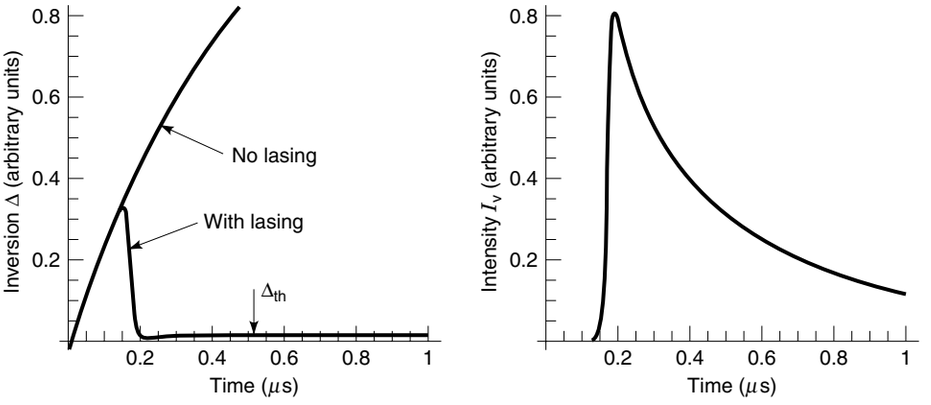

Figure 5. Solution of the laser rate equations for the inversion and laser intensity for a high gain, low optical loss system where chemical pumping of the upper laser level is initiated at $t = 0$.

dia and greater geometrical scaling for high-power performance.

The inversion Δ is established via the pumping process, as shown schematically in Fig. 1(d), and the time dependence of the population inversion is described by the generic laser rate equations:

$$\begin{aligned}
\frac{dN_2}{dt} &= R_{p2} - \Gamma_2 N_2 - \sigma \left(N_2 - \frac{g_2}{g_1} N_1 \right) (I_\nu / h\nu) \\
\frac{dN_1}{dt} &= R_{p1} + \Gamma_{21} + \sigma \left(N_2 - \frac{g_2}{g_1} N_1 \right) (I_\nu / h\nu) - \Gamma_1 \\
\frac{dI_\nu}{dt} &= A_{21} N_2 \left(\frac{V g(\lambda)}{V_m \rho(\lambda)} \right) + c\sigma \left(N_2 - \frac{g_2}{g_1} N_1 \right) (I_\nu) - \alpha c I_\nu
\end{aligned} \tag{7}$$

The rate R_{p2} for chemical production of the upper laser level will depend on the concentration of reagents and is specific to the chemical reaction employed. The chemical pumping reactions may also generate some population in the lower laser level. The rate for this undesirable process is R_{p1}. The decay rates Γ_1 and Γ_2 include all radiative and collisional processes that remove population from the upper and lower laser levels, respectively. Any process that moves population from the upper laser level to the lower laser level is represented by the decay rate Γ_{21}. The intensity of laser radiation inside the laser cavity, I_ν, grows initially from the spontaneous emission into a specific cavity mode with volume V_m, represented by the first term in the equation for dI_ν/dt. The mode density is $\rho(\lambda) = 8\pi/c\lambda^2$. The second and third terms in the laser intensity equation represent laser amplification due to stimulated emission and loss of photons from the laser cavity, respectively.

An example solution to the laser rate equations (7) is shown in Fig. 5. The chemical pumping rate begins suddenly at $t = 0$ and the population inversion increases rapidly. The inversion reaches threshold almost immediately, as the losses for this system are low. The population inversion, $\Delta = N_2 - N_1$, for the two cases, (1) no stimulated emission and (2) with lasing, are both shown. The lasing is delayed by $t = 0.2$ μs as the photons circulate between the mirrors until a large pulse is achieved. During lasing, the inversion is rapidly depleted by stimulated emission and maintained at the threshold value. The intensity of the laser pulse decays at longer times as initial reagents are consumed and population in the lower laser level increases. Most chemical lasers are continuous-wave (cw) or steady-state devices in which reagents are continually replenished in a flowing system. Under such conditions the laser intensity quickly achieves a steady value.

The requirements for pump rates of a chemical laser can be understood from a steady-state analysis of the rate equations (7). For a molecular system with many accessible rotational levels, pump rates of 10^{19} molecules/cm$^3 \cdot$ s are required to achieve a gain of greater than 0.1%/cm in the visible portion of the spectrum, $\lambda \sim 500$ nm. For a bimolecular pumping reaction with a nearly gas kinetic rate coefficient, the product of reagent concentrations required to achieve this pump rate is approximately 10^{29} molecules^2/cm^6. These rapid excitation rates are often limited by diffusion of reagents in a supersonic mixing nozzle. If the time scale for mixing is long compared with the radiative lifetime, then the effective excitation rate is reduced and the required reagent concentrations are increased. Current nozzle technology limits the mixing time to values greater than 1 μs to 10 μs.

The power output from the laser depends on many factors, including the energy density created by the pump reaction, laser gain and losses, output coupling, and the saturation intensity. For example, the output power as a function of mirror reflectivity is shown in Fig. 6 for a system with low gain and

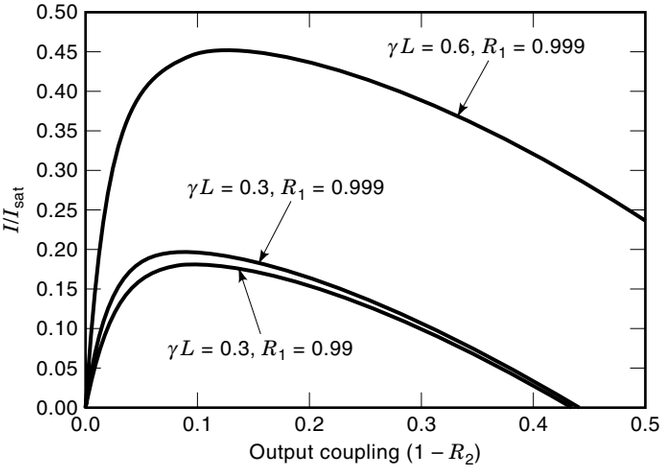

Figure 6. A Rigrod analysis (see Ref. 18) of the laser intensity as a function of output mirror reflectivity, R_2, for several values of gain and optical losses at the second mirror with maximum reflectivity, R_1.

high saturation intensity. The saturation intensity is dependent only on parameters of the gain media:

$$I_{sat} = (hc/\lambda)/(\sigma/\Gamma_2) \tag{8}$$

Clearly there is an optimum output coupling (mirror reflectivity) to achieve maximum laser output power that depends on gain, losses, and saturation intensity.

Two key laser performance parameters describing the output power are mass efficiency σ_m (kJ/kg) and nozzle flux δ (kW/cm^2). The mass efficiency describes the laser power achieved per reagent flow rate and is particularly important for space-based applications where the cost of delivering fuel to orbit can dominate total system costs. Typical mass efficiencies for HF lasers are ~150 kJ/kg and for chemical oxygen–iodine laser devices, ~300 kJ/kg. By comparison, dynamite (TNT) possesses an energy density of 9 MJ/kg. The nozzle flux parameter represents the laser power achieved per unit cross-sectional area of the nozzle assembly. This is a key parameter for power scaling and specifies the size of a high-power chemical laser.

Beam quality is a key parameter that describes the ability to propagate the laser as a narrow beam and to focus the beam to a small spot. The angular divergence of a laser beam, $\theta_{1/2}$, is ultimately limited by diffraction, $\theta_{1/2} \sim (\lambda/D)$, where D is the diameter of the limiting aperture or cavity mirror. However, such a diffraction-limited beam is not achieved, and the beam quality (BQ) is often reported as the ratio of the actual spot size to the diffraction-limited spot size. Chemical lasers, particularly the chemical oxygen–iodine laser (COIL) device, have very good beam quality, due to the transport of excess heat from the laser cavity via the supersonic flow. Beam quality for a chemical laser is typically limited by the spatial uniformity of the gain media imposed by the supersonic mixing nozzles.

The ability of a laser to damage a distant target is often characterized by the source brightness or power per unit solid angle of beam divergence. The brightness B for a diffraction-limited beam is approximately related to laser power P, operating wavelength λ, and diameter of the laser aperature, D:

$$B = PD^2/\pi\lambda^2 \tag{9}$$

It is the power flux or power per unit area that causes damage due to rapid heating, and the area to which a laser beam can be focused is limited by diffraction, beam quality, and beam jitter. Device powers of multimegawatts and brightnesses of 10^{20} W/sr to 10^{23} W/sr are required for some military missions (5).

THE METASTABLE-ENERGY-TRANSFER CHEMICAL LASER

To extend chemical laser operation to significantly shorter wavelengths than the HF or DF laser requires a system that establishes an inversion between the more energetic electronic states of an atom or molecule. There are several advantages to shorter-wavelength chemical lasers, including higher power per mass of reagents and reduced beam divergence due to diffraction at the limiting aperture (6). Rather than depositing excess reaction energy into the stretching of the newly formed bond (vibration), the chemical reaction could yield

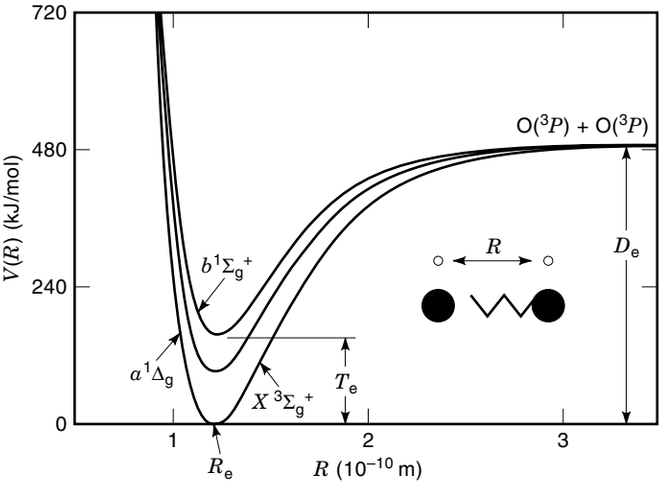

Figure 7. Morse potential energy curves for the three lowest electronic states of molecular oxygen, which dissociate to ground-state oxygen atoms, O(^3P). The dissociation energy, D_e, for the ground state, $X\ ^3\Sigma_g^+$, and the electronic energy, T_e, for the second excited state, $b^1\Sigma_g^+$, are indicated.

atoms or molecules with internal excitation of the electrons. For example, molecular oxygen has two excited electronic states with electronic energy of T_e = 95 kJ/mol and 158 kJ/mol above the ground electronic state (7), as shown in the potential energy curves of Fig. 7. To understand these curves, consider the oxygen molecule as two masses connected by a spring, where the bonding electrons shared by the two oxygen atoms provide the restoring force. As the oxygen molecule vibrates, the distance between the two oxygen atoms, R, changes between the two extremes, and the potential energy curve represents this range in internuclear separation at various energies, V. At large enough vibrational energy, the internuclear separation becomes quite large and the molecule dissociates to two ground-state oxygen atoms. The curve labeled $X\ ^3\Sigma_g^+$ is the lowest electronic state of molecular oxygen, which has a dissociation energy of D_e = 489 kJ/mol and a bond length of R_e = 0.1207 nm. If the electron cloud around the oxygen molecule is excited, then the effective spring force constant is changed, and the excited electronic states, labeled $a\ ^1\Delta_g$ and $b\ ^1\Sigma_g^+$, are generated.

To produce an inversion between electronic states efficiently requires the chemical reaction to selectively produce a specific excited electronic state over all other states, particularly the ground electronic state. Reactions involving light atoms and molecules tend to preserve the total electronic spin. Thus, the generation of an electronic inversion is aided by a difference in electronic spin between the ground and excited electronic states. However, such transitions exhibit slow spontaneous emission rates and thus very low stimulated emission cross sections and insufficient gain to build a laser. For example, the $a\ ^1\Delta$–$X\ ^3\Sigma$ transition in O_2 shown in Fig. 5 exhibits a particularly slow spontaneous emission rate of 2.58×10^{-4} s^{-1} (8). However, these long-lived, or metastable, electronically excited states establish a large energy reservoir that could be used to pump a chemical laser. By collisionally transferring the energy stored in these metastable states to a suitable lasant species, a new class of chemical laser, the

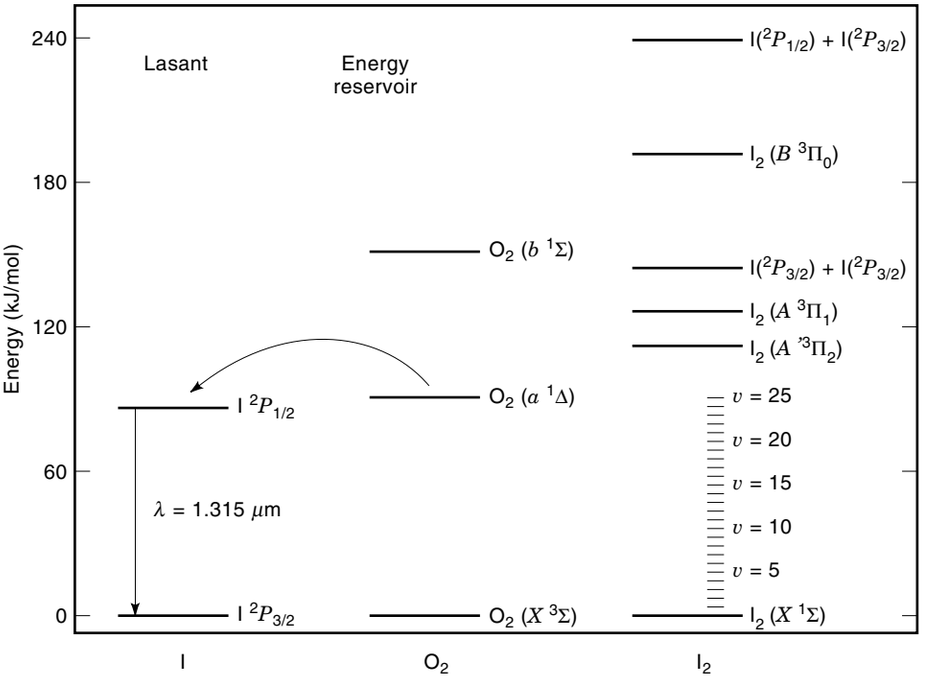

Figure 8. Energy-level diagram for the COIL illustrating the resonant energy transfer from metastable reservoir $O_2(a\ ^1\Delta)$ to the upper laser level of atomic iodine, $I(^2P_{1/2})$. The energy levels for several key states involved in the dissociation of molecular iodine are also provided.

metastable energy transfer chemical laser, can be developed. The chemical oxygen–iodine laser is the prime example of such a energy transfer laser.

THE CHEMICAL OXYGEN–IODINE LASER

The chemical oxygen–iodine laser (COIL) was first demonstrated at the Air Force Weapons Laboratory in 1977 (9). The first electronically excited state of molecular oxygen, $O_2(a\ ^1\Delta)$ (see Fig. 7), is produced by a two-phase reaction of chlorine gas and liquid basic hydrogen peroxide with near 100% efficiency. Once produced, this singlet state of oxygen can be transported for considerable distances even at moderately high pressures, as the radiative lifetime is ~64 min and $O_2(a\ ^1\Delta)$ is very resistant to collisional deactivation. Thus, $O_2(a\ ^1\Delta)$ is a metastable-energy reservoir. Energy densities of 10 kJ/m^3 to 20 kJ/m^3 are typically attained. However, the long radiative lifetime leads to exceptionally low gain, and direct lasing on the $O_2(a\ ^1\Delta$–$X\ ^3\Sigma)$ magnetic dipole transition is not achievable.

The chemical oxygen–iodine laser operates on an inversion between the $^2P_{1/2}$ and $^2P_{3/2}$ spin-orbit-split states of atomic iodine at a wavelength of 1.315 μm. A near resonance exists between $O_2(a\ ^1\Delta)$ and $I(^2P_{1/2})$ with an energy difference of only 3.3 kJ/mol, and laser pumping is achieved by collisional energy transfer from the $O_2(a\ ^1\Delta)$ metastable energy reservoir, as shown in Fig. 8. The energy transfer is rapid and a near-equilibrium condition between the upper laser level, $I(^2P_{1/2})$, and $O_2(a\ ^1\Delta)$ is quickly established:

$$O_2(a\ ^1\Delta) + I(^2P_{3/2}) \leftrightarrow O_2(X\ ^3\Sigma) + I(^2P_{1/2}) \tag{10}$$

The ratio of excited- and ground-state atomic iodine concentrations is approximately determined by the equilibrium constant for reaction equation (10), $K_{eq} = 0.75 \exp(402/T)$:

$$\frac{[I(^2P_{1/2})]}{[I(^2P_{3/2})]} = \frac{[O_2(a\ ^1\Delta)]}{[O_2(X\ ^3\Sigma)]} K_{eq}(T) \tag{11}$$

where the brackets [ ] indicate concentration of the species.

The atomic iodine $^2P_{1/2} \rightarrow {}^2P_{3/2}$ lasing transition is composed of six hyperfine components, as shown in Fig. 9. The nuclear spin is $I = \frac{5}{2}$. The $^2P_{1/2}(F' = 3) \rightarrow {}^2P_{3/2}(F'' = 4)$ component provides the highest gain and lasing occurs on this individual transition. Note that the degeneracies of the hyperfine components are $g_F = 2F + 1$, so that the degeneracy of the upper and lower laser levels are $g_2 = 7$ and $g_1 = 9$, respectively. If all the hyperfine levels are populated statistically,

$$\begin{aligned}[I(^2P_{1/2}, F' = 3)] &= \frac{7}{12}[I(^2P_{1/2})] \\ [I(^2P_{3/2}, F'' = 4)] &= \frac{9}{24}[I(^2P_{3/2})]\end{aligned} \tag{12}$$

then the population inversion is

$$\begin{aligned}\Delta &= [I(^2P_{1/2}, F' = 3)] - \frac{g_2}{g_1}[I(^2P_{3/2}, F'' = 4)] \\ &= \frac{7}{12}([I(^2P_{1/2})] - 0.5[I(^2P_{3/2})]) \\ &= \frac{7}{12}\left\{K_{eq}\left(\frac{Y}{1-Y}\right) - \frac{1}{2}\right\}[I(^2P_{3/2})]\end{aligned} \tag{13}$$

where the yield

$$Y = \text{yield} = \frac{[O_2(a\ ^1\Delta)]}{[O_2(X\ ^3\Sigma)] + [O_2(a\ ^1\Delta)]} \tag{14}$$

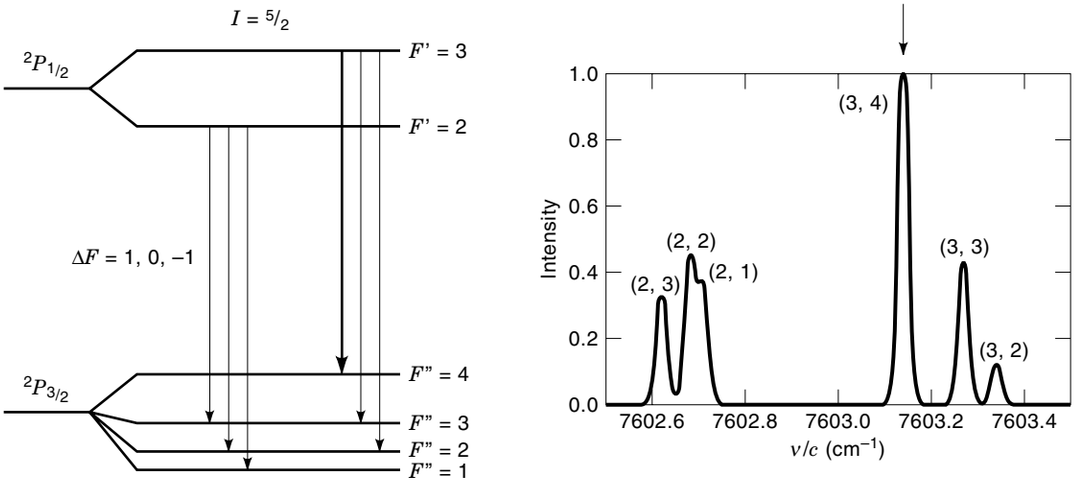

Figure 9. Hyperfine structure and spectrum of the I($^2P_{1/2} \rightarrow {}^2P_{3/2}$) transition in atomic iodine indicating the greatest gain is achieved for the $F' = 3 \rightarrow F'' = 4$ component near $\nu = 7603.2$ cm^{-1} or $\lambda = 1.315$ μm. The spectrum is simulated using line shapes of Eq. (5) with a linewidth of $\Delta\nu_D = 840$ MHz.

The threshold for lasing (positive inversion) is achieved at $T = 295$ K when the ratio of $O_2(a\ ^1\Delta)$ to total oxygen, or yield of singlet oxygen, is approximately 15%. The threshold is reduced considerably at lower temperatures due to the temperature dependence of the equilibrium constant. At $T = 160$ K, a temperature consistent with typical nozzle exit conditions, the threshold yield is reduced to 5%. The cross section for stimulated emission at room temperature is $\sigma = 7.4 \times 10^{-18}$ cm^2 (5) and the gain in a COIL device is typically near $\gamma = 1\%$/cm.

A schematic diagram of a typical supersonic COIL device is shown in Fig. 10. The chemical generator of $O_2(a\ ^1\Delta)$ is a two-phase reactor governed by the stoichiometry:

$$Cl_2(g) + H_2O_2(l) + 2KOH(l) \rightarrow O_2(a\ ^1\Delta) + 2KCl + 2H_2O \quad (15)$$

The KOH/H_2O_2 solution is termed the basic hydrogen peroxide solution (BHP). The alkali-metal hydroxide (KOH) is required to form the hydroperoxide ion (O_2H^-):

$$KOH \rightarrow K^+ + OH^- \quad (16)$$

$$OH^- + H_2O_2 \rightarrow O_2H^- + H_2O \quad (17)$$

The favored reaction mechanism for the production of singlet oxygen involves four steps:

$$O_2H^- + Cl_2 \rightarrow HOOCl + Cl^- \quad (18)$$

$$O_2H^- + HOOCl \rightarrow ClO_2^- + H_2O_2 \quad (19)$$

$$ClO_2^- \rightarrow O_2(a\ ^1\Delta) + Cl^- \quad (20)$$

$$O_2(a\ ^1\Delta) \rightarrow O_2(X\ ^3\Sigma) \quad (21)$$

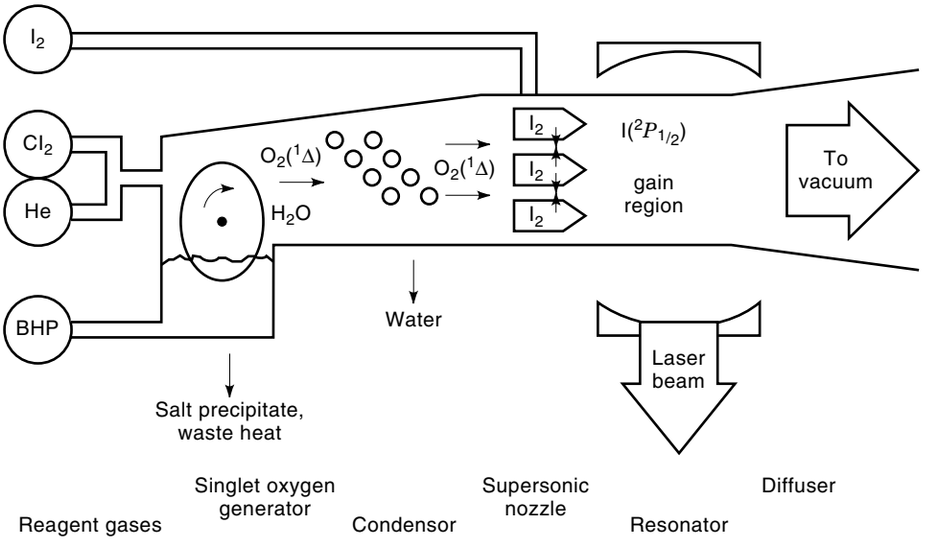

Figure 10. Schematic diagram of a typical supersonic COIL.

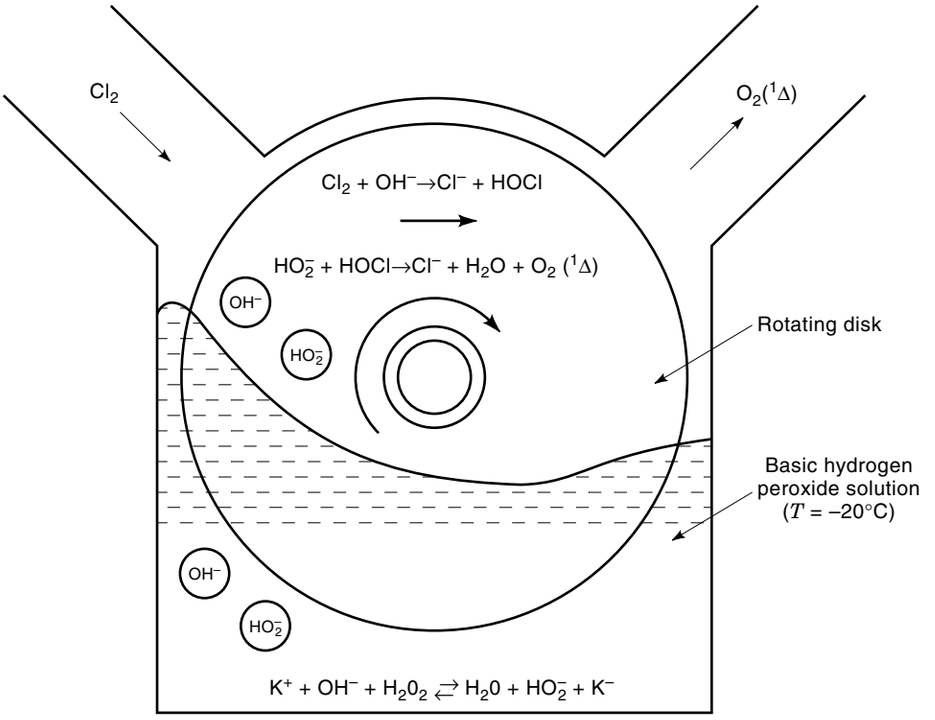

Figure 11. Rotating disk design for the chemical generation of singlet oxygen, $O_2(a\ ^1\Delta)$, via the two-phase reaction of chlorine gas with liquid hydrogen peroxide (from Ref. 10).

The earliest singlet oxygen generators were of a sparger design, where chlorine gas is bubbled through the liquid hydrogen peroxide solution. The two-phase reaction requires large liquid surface to volume ratios for efficient operation, and the second generation of chemical generators were based on a wetted wall reactor, as shown in Fig. 11 (10). By rotating a stack of disks through a pool of basic hydrogen peroxide and past a stream of chlorine gas, the reaction is confined to a thin film on each disk. The time required to diffuse the singlet oxygen from within the liquid phase to the gas-phase interface is reduced and the deactivation of $O_2(a\ ^1\Delta)$ via reaction Eq. (21) is minimized. Advanced generators involving sprays of droplets with near-uniform size are now being used for COIL devices.

The effluent from the singlet oxygen generator includes $O_2(a\ ^1\Delta)$ and water vapor. Water vapor is an efficient collisional quencher of the upper laser level, $I(^2P_{1/2})$, and reduces device performance. Thus a water trap or condenser is used to remove the water from the gas stream. The total pressure at the exit of the generator is typically 1.5 kPa to 6.5 kPa and usually includes helium as a diluent.

Molecular iodine is injected transverse to the primary oxygen flow near the throat of a supersonic nozzle, as shown in Fig. 12 (10). The molecular iodine is rapidly dissociated to atomic iodine by the presence of the singlet oxygen in a complex, multistep mechanism so that the flow is fully dissociated as it reaches the exit plane of the nozzle and before entering the gain region.

The iodine dissociation process is poorly understood and provides the greatest difficulty in modeling the gas-phase kinetics of the COIL device. The energetics of the dissociation process are shown in Fig. 8. The second electronically excited state of oxygen, $O_2(b\ ^1\Sigma)$, is produced from the energy-pooling reaction:

$$O_2(a\ ^1\Delta) + O_2(a\ ^1\Delta) \rightarrow O_2(b\ ^1\Sigma) + O_2(X\ ^3\Sigma) \qquad (22)$$

and $O_2(b\ ^1\Sigma)$ is sufficiently energetic to dissociate iodine. However, there is insufficient concentration of $O_2(b\ ^1\Sigma)$ to explain the phenomenological dissociation rate, particularly when significant water vapor is present. A slow initiation of the dissociation process may begin by $O_2(a\ ^1\Delta)$ excitation of vibrationally excited iodine, I_2^*, followed by a second $O_2(a\ ^1\Delta)$

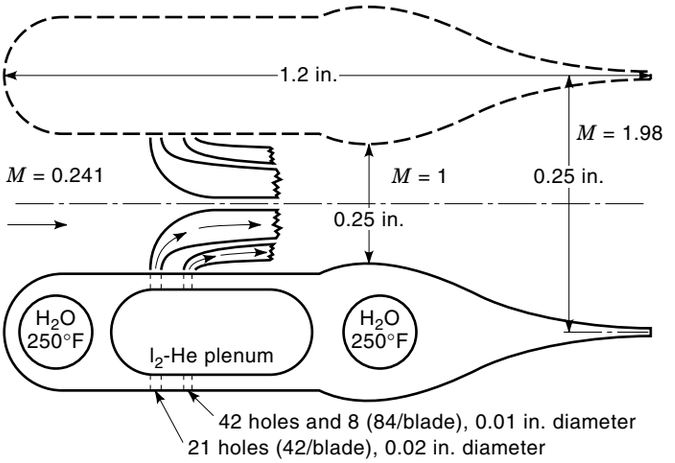

Figure 12. Typical supersonic mixing nozzle for a COIL where molecular iodine is injected transverse to the flow of singlet oxygen (from Ref. 10).

Table 2. Simplified COIL Kinetic Mechanism

Reaction	Rate Coefficient (cm^3/molecules · s)
$O_2(a\ ^1\Delta) + O_2(a\ ^1\Delta) \rightarrow O_2(b\ ^1\Sigma) + O_2(X\ ^3\Sigma)$	2.7×10^{-17}
$O_2(b\ ^1\Sigma) + H_2O \rightarrow O_2(a\ ^1\Delta) + H_2O$	6.7×10^{-12}
$I_2(X\ ^1\Sigma) + O_2(b\ ^1\Sigma) \rightarrow I(^2P_{3/2}) + I(^2P_{3/2}) + O_2(X\ ^3\Sigma)$	4.0×10^{-12}
$I_2(X\ ^1\Sigma) + O_2(a\ ^1\Delta) \rightarrow I_2^* + O_2(X\ ^3\Sigma)$	7.0×10^{-15}
$I_2(X\ ^1\Sigma) + I(^2P_{1/2}) \rightarrow I_2^* + I(^2P_{3/2})$	3.8×10^{-11}
$I_2^* + O_2(a\ ^1\Delta) \rightarrow I(^2P_{3/2}) + I(^2P_{3/2}) + O_2(X\ ^3\Sigma)$	3.0×10^{-10}
$I_2^* + H_2O \rightarrow I_2(X\ ^1\Sigma) + H_2O$	3.0×10^{-10}
$I(^2P_{3/2}) + O_2(a\ ^1\Delta) \rightarrow I(^2P_{1/2}) + O_2(X\ ^3\Sigma)$	7.8×10^{-11}
$I(^2P_{1/2}) + O_2(X\ ^3\Sigma) \rightarrow I(^2P_{3/2}) + O_2(a\ ^3\Delta)$	2.7×10^{-11}
$I(^2P_{1/2}) + O_2(a\ ^1\Delta) \rightarrow I(^2P_{3/2}) + O_2(b\ ^1\Sigma)$	1.1×10^{-13}
$I(^2P_{1/2}) + H_2O \rightarrow I(^2P_{3/2}) + H_2O$	2.0×10^{-12}

collision producing ground-state atomic iodine. The resulting iodine atoms are rapidly excited to the spin-orbit state, $I(^2P_{1/2})$, by energy transfer. The dissociation then rapidly accelerates as $I(^2P_{1/2})$ replaces $O_2(a\ ^1\Delta)$ as the dominant partner for production of I_2^*. This dissociation process removes at least 2, and sometimes as many as 6 to 18, $O_2(a\ ^1\Delta)$ molecules per dissociated I_2 molecule, depending on the rate for deactivating the intermediate, I_2^*, and any quenching of $I(^2P_{1/2})$. In order to avoid consuming a large fraction of the energy stored in the metastable reservoir in this dissociation process, the ratio of molecular iodine to singlet oxygen flow rates is usually small, about 1%. During the lasing process, the iodine atoms will experience many energy transfer excitation and stimulated emission cycles to extract most of the energy stored in $O_2(a\ ^1\Delta)$.

A simplified kinetic mechanism that retains the essential features of the iodine dissociation process is provided in Table 2. A complete review of the gas-phase kinetics of the COIL was conducted in 1987 (11). The transverse injection of iodine into the throat of the supersonic mixing nozzle significantly complicates the iodine dissociation process, as discussed in Ref. (12).

In the gain region, the molecular iodine is fully dissociated and a near-equilibrium between excited iodine atoms and $O_2(a\ ^1\Delta)$ is rapidly attained via the energy transfer reaction (10). Quenching of $I(^2P_{1/2})$ by H_2O drains energy from the singlet oxygen reservoir, until stimulated emission dominates the deactivation. Continuous-wave lasing action is achieved on a single hyperfine transition of the inhomogeneously broadened iodine atom at $\lambda = 1.315\ \mu m$.

SHORT WAVELENGTH CHEMICAL LASER

Significant progress toward the development of chemically driven laser operating in the visible portion of the spectrum has been made over the past few years. The promise of very high brightness, high mass efficiency, and wavelength agility has justified a modest basic research program for several decades (6). For example, Eq. (9) suggests that a chemical laser operating in the blue would possess a diffraction limited brightness of almost 40 times that for an HF laser with similar power and aperture.

The premier candidate for a metastable energy reservoir to drive a visible chemical laser is $NF(a\ ^1\Delta)$, which possesses an energy of 1.4 eV per molecule and has a radiative lifetime of 5.6 s. Energy densities of greater than 6.7 J/L have been demonstrated with near unit chemical production efficiency. The two primary methods of production are the reaction of hydrogen atoms with NF_2, and the thermal decomposition of fluorine azide.

To extract the energy stored in $NF(a\ ^1\Delta)$ in the form of laser power, energy transfer to lasant species such as BiF, $NF(b\ ^1\Sigma)$, $IF(B\ ^3\Pi)$, and $BH(A\ ^1\Pi)$ have been studied. In a pulsed thermolysis apparatus, BiF(A) concentrations of 1.8×10^{13} molecules/cm^3 have been achieved and a gain of 0.027%/cm demonstrated in the blue. Stimulated emission has been observed in a Mach 2.5 tabletop shock tube (13). However, saturated lasing has not been demonstrated. A bibliography summarizing the research toward demonstrating a short wavelength chemical laser has been published (14).

THE AIRBORNE LASER

The potential for employing high-power chemical lasers as a military weapon was recognized soon after the early laser demonstrations in the 1960s. Indeed, the development of the chemical laser is strongly tied to such applications, and a broad research and development activity across many US federal agencies continues through today. The Airborne Laser Laboratory (ALL) developed in the 1970s and early 1980s was the first major demonstration of the potential for high-power lasers as airborne weapons. A 500 kW carbon dioxide gas dynamic laser combined with an accurate pointing and tracking system was tested aboard a modified NKC-135 aircraft. In May of 1983, the ALL destroyed five AIM-9 "Sidewinder" missiles at the Naval Weapons Center Range at China Lake, California. A thorough history of the ALL program has been documented in *Airborne Laser: Bullets of Light* (15).

The Strategic Defense Initiative (SDI) announced by President Reagan in March of 1983 envisioned the use of high-power space-based lasers for strategic defense against ballistic missile attack (5). A prime advantage the laser offers for missile defense is its ability to deliver lethal energy to very distant targets at the speed of light. The HF-DF chemical laser, the excimer laser, and the free-electron laser were investigated intensively under the SDI program.

In 1996, the Air Force contracted to develop a megawatt class COIL mounted aboard a modified Boeing 747-400F capable of destroying theater missiles during the powered boost phase. This new major weapons system, the Airborne Laser (ABL), is designed to destroy multiple tactical ballistic missiles, possibly carrying chemical and biological weapons, launched from random, previously unidentified sites over enemy territory at ranges of several hundred kilometers. The ABL is the first directed-energy major defense acquisition program. Such technology offers to revolutionize warfare, as expressed by Secretary of the Air Force Sheila E. Widnall in 1997 (16):

> It isn't very often an innovation comes along that revolutionizes our operational concepts, tactics, and strategies. You can probably name them on one hand—the atomic bomb, the satellite, the jet engine, stealth, and the microchip. It's possible the airborne laser is in this league.

A fleet of seven Airborne Laser aircraft are anticipated to become operational by the year 2008.

The chemical oxygen–iodine laser also has several important industrial applications (17). Materials processing, including metal-cutting operations, has been demonstrated. The wavelength of the COIL device is ideal for transmission through fiber optics, which may be an appropriate approach for beam delivery in an industrial setting.

CONCLUSIONS

The universe is filled with light and much that we know about the world around us is derived from the interaction of electromagnetic radiation with matter. Indeed, there are 100 million photons for every massive particle in the universe. With the advent of the laser a new source of light is available that possesses unique monochromatic, coherence, and propagation characteristics. When such laser devices are driven by chemical reactions, the power of the laser beam can be spectacular. Many scientific and technical challenges have been met in the past three decades, integrating advances in chemistry, physics, fluid dynamics, optics, and engineering to develop these high-power chemical lasers. These devices are now finding important applications in industrial and military operations.

BIBLIOGRAPHY

1. J. C. Polanyi, Proposal for an infrared maser dependent on vibrational excitation, *J. Chem. Phys.,* **34**: 347, 1961.
2. R. W. F. Gross and J. F. Bott (ed.), *Handbook of Chemical Lasers.* New York: Wiley, 1976.
3. J. B. Anderson, *Adv. Chem. Phys.,* **41**: 229, 1980.
4. J. V. V. Kasper and G. C. Pimentel, HCl chemical laser, *Phys. Rev. Lett.,* **14**: 352, 1965.
5. N. Bloembergen and C. K. N. Patel (eds.), Report to the American Physical Society Study Group on the Science and Technology of Directed Energy Weapons, *Rev. Mod. Phys.,* **59** (3), Part II: S33–S47, 1987.
6. G. P. Perram, Visible chemical lasers, in *Proceedings of the International Conference on LASERS '89,* McLean, VA: STS Press, 1990, pp. 232–240.
7. G. Herzberg, Molecular Spectra and Molecular Structure. I. Spectra of Diatomic Molecules, New York: Van Nostrand Reinhold, 1950.
8. R. M. Badger, A. C. Wright, and R. F. Whitlock, Absolute intensities of the discrete and continuous absorption bands of oxygen gas at 1.26 and 1.065 μm and the radiative lifetime of the singlet-delta state of oxygen, *J. Chem. Phys.,* **43**: 4345, 1965.
9. W. E. McDermott et al., An Electronic Transition Chemical Laser, *App. Phys. Lett.,* **32**: 469, 1978.
10. K. A. Truesdell, C. A. Helms, and G. D. Hager, A History of COIL Development in the USA, in *SPIE Proceedings of the 10th International Symposium on Gas Flow and Chemical Lasers,* **2802**: 217–237, 1995.
11. G. P. Perram, Approximate Analytical Solution for the Dissociation of Molecular Iodine in the Presence of Singlet Oxygen, *Intl. J. Chem. Kinetics,* **27**: 817–828, 1995.
12. J. A. Miller and E. J. Jumper, Role of mixing in the Chemical Oxygen–Iodine Laser reactions, *AIAA J.,* **32**: 1228–1233, 1994.
13. D. J. Benard and E. Boehmer, Chemically pumped visible-wavelength laser with high optical gain, *Appl. Phys. Lett.,* **65**: 1340–1342, 1994.
14. G. P. Perram, The challenges of inexpensive laser demonstrations, in *Proc. Int. Conf. LASERS '92,* McLean, VA: STS Press, 1993, pp. 158–165.
15. R. W. Duffner, *Airborne Laser: Bullets of Light,* New York: Plenum Trade, 1997.
16. P. McKenna, Set Lasers on Stun!, *Airman,* **41**: 10–13, 1997.
17. A. Kar, J. E. Scott, and W. P. Latham, Effects of mode structure on three-dimensional laser heating due to single or multiple rectangular beams, *J. Appl. Phys.,* **80**: 667–674, 1996.
18. J. T. Verdeyen, *Laser Electronics,* 2nd ed., Englewood Cliffs, NJ: Prentice Hall, 1989.

Reading List

N. G. Basov et al., *Chemical Lasers,* Berlin: Springer, 1990.

G. E. Forden, The Airborne Laser, *IEEE Spectrum,* **34** (9): 40–49, 1997.

G. C. Pimentel, Chemical Lasers, *Sci. Am.,* **214**: 32–39, April 1966.

H. F. Schaefer III, The F + H_2 Potential Energy Surface: The Ecstasy and the Agony, *J. Phys. Chem.,* **89**: 5336, 1985.

A. L. Schawlow, Laser Light, *Sci. Am.,* **219**: 120–136, September 1968.

K. A. Truesdell and S. E. Lamberson, Phillips Laboratory COIL Technology Overview, in *SPIE Proc. 9th Int. Symp. Gas Flow Chem. Lasers,* **1810**: 1992, pp. 476–492.

GLEN P. PERRAM
Air Force Institute of Technology